agronomy

MDPI

Article

Chemical and Microbial Characteristics of Blackening Disease in Lotus (*Nelumbo nucifera* Gaertn.) Caused by *Hirschmanniella diversa* Sher

Hazuki Kurashita [1,2], Kyohei Kuroda [1,*], Shinya Maki [2], Takeshi Sato [3], Motonori Takagi [4], Maki Goto [5], Tetsuro Kariya [4], Masashi Hatamoto [3], Takashi Yamaguchi [2], Shun Tomita [1] and Takashi Narihiro [1]

1 Bioproduction Research Institute, National Institute of Advanced Industrial Science and Technology (AIST), 2-17-2-1 Tsukisamu-Higashi, Toyohira-ku, Sapporo 062-8517, Hokkaido, Japan; s205003@stn.nagaokaut.ac.jp (H.K.); tomita.s@aist.go.jp (S.T.); t.narihiro@aist.go.jp (T.N.)
2 Department of Science of Technology Innovation, Nagaoka University of Technology, 1603-1, Kami-tomioka, Nagaoka 940-2188, Niigata, Japan; maki@vos.nagaokaut.ac.jp (S.M.); ecoya@vos.nagaokaut.ac.jp (T.Y.)
3 Department of Civil and Environmental Engineering, Nagaoka University of Technology, 1603-1, Kami-tomioka, Nagaoka 940-2188, Niigata, Japan; s205036@stn.nagaokaut.ac.jp (T.S.); hatamoto@vos.nagaokaut.ac.jp (M.H.)
4 Horticultural Research Institute, Ibaraki Agricultural Center, 3165-1 Ago, Kasama 319-0292, Ibaraki, Japan; mo.takagi@pref.ibaraki.lg.jp (M.T.); t.kariya@pref.ibaraki.lg.jp (T.K.)
5 Tsuchiura Agricultural Extension Center, 5-17-26 Manabe, Tsuchiura 300-0051, Ibaraki, Japan; ma_gotou@pref.ibaraki.lg.jp
* Correspondence: k.kuroda@aist.go.jp; Tel.: +81-11-857-8402

check for updates

Citation: Kurashita, H.; Kuroda, K.; Maki, S.; Sato, T.; Takagi, M.; Goto, M.; Kariya, T.; Hatamoto, M.; Yamaguchi, T.; Tomita, S.; et al. Chemical and Microbial Characteristics of Blackening Disease in Lotus (*Nelumbo nucifera* Gaertn.) Caused by *Hirschmanniella diversa* Sher. *Agronomy* **2021**, *11*, 2517. https://doi.org/10.3390/agronomy11122517

Academic Editor: Erin N. Rosskopf

Received: 5 November 2021
Accepted: 9 December 2021
Published: 11 December 2021

Publisher's Note: MDPI stays neutral with regard to jurisdictional claims in published maps and institutional affiliations.

Copyright: © 2021 by the authors. Licensee MDPI, Basel, Switzerland. This article is an open access article distributed under the terms and conditions of the Creative Commons Attribution (CC BY) license (https://creativecommons.org/licenses/by/4.0/).

Abstract: The lotus (*Nelumbo nucifera* Gaertn.) is widely cultivated in Asia, but a blackening disease in the lotus tuber, called "*kurokawa-senchu-byo*", is a serious problem caused by the *Hirschmanniella diversa* Sher plant-parasitic nematode. To effectively control the disease, we must elucidate the blackening mechanisms; therefore, in this study, we performed a soil chemical analysis and an evaluation of the disease level in the lotus cultivation fields, identified the chemical components of the black spots on the lotus surface, and performed a 16S rRNA gene-based microbial community analysis of the black spots. Using linear regression analysis, a positive linear relationship with a strong correlation between the damage index values and fertilizer components such as P_2O_5 was observed. As a result of scanning electron microscopy and energy-dispersive X-ray spectroscopy analysis, phosphorus (P) and iron (Fe) were found to be concentrated in the black spots of the lotus tubers. Furthermore, we found that the concentrations of P and Fe in the black spots were 1.5- and 2.7-fold higher, respectively, than those found in the healthy parts of the lotus tubers. A 16S rRNA gene analysis revealed that dissimilatory Fe(III)-reducing bacteria (DIRB) were predominant in the black spots, suggesting that these bacteria are important to the formation of P and Fe compounds in the black spots.

Keywords: "*kurokawa-senchu-byo*"; lotus root; plant-parasitic nematode; dissimilatory Fe(III)-reducing bacteria (DIRB); damage index; iron; phosphorus

1. Introduction

The lotus (*Nelumbo nucifera* Gaertn.) is widely cultivated in Asia, and the cultivation areas are estimated to be 133,300 ha in China and 4000 ha in Japan [1,2]. Recently, the "*kurokawa-senchu-byo*" of lotus tubers has become a serious problem in Japan and China as a result of continuous monocropping [3]. The disease causes blackening and deformation of the lotus tubers [1,4], and a resulting annual economic loss is estimated at USD 1 million in the Tokushima Prefecture (the second-largest lotus production area in Japan). It is known that the disease has been caused by two plant-parasitic nematodes, *Hirschmanniella diversa* Sher and *H. imamuri* Sher [5]. A recent study revealed that *H. diversa* is a more critical

causative agent of the disease than *H. imamuri,* based on quantitative PCR approaches [1,6]. *H. diversa* is known to exhibit root-parasitic nematodes that may have a wide range of plant hosts since it has been detected in several types of weeds [7]. Based on microscopic approaches, several stages of the nematodes (e.g., adults, juveniles, and eggs) were found in the lotus roots, suggesting that *H. diversa* completes most of its lifecycle in the roots [8].

While calcium cyanamide is the only pesticide available in Japan for the control of *H. diversa*, there are reports of fields where the damage index of the lotus often has not decreased, despite the application of this pesticide [1]. In a recent study, several nematicides were screened to develop an effective nematode-management system [9]. As a result, benfuracarb was recommended as the most effective nematicide for *H. diversa* control. In July 2020, a new benfuracarb-based nematicide was registered in Japan, and it is expected to control *H. diversa* in lotus cultivation fields [10]. Furthermore, the authors proposed a new integrated pest-management program, which indicates the importance of using a combination of a benfuracarb-based nematicide, weed control, and calcium cyanamide applications, depending on the extent of the damage, for the control of "*kurokawa-senchu-byo*".

Although the elucidation of the blackening mechanisms of "*kurokawa-senchu-byo*" is important for its control, until now, only limited studies have been reported. Takagi et al. elucidated the life cycle of *H. diversa* and found that the peak seasonal breeding period occurred from April to mid-May, with the possibility of overwinter by fourth-stage juveniles or adults in lotus roots, weeds, and soil [4]. Uematsu et al. confirmed that *H. diversa* could penetrate to a depth of approximately 1 mm into young lotus tuber apices for 24 h and, based on microscopic approaches, suggested that *H. diversa* produces digestive enzymes. In addition, the authors proposed that the penetrating sites of young lotus tuber apices become blackened due to oxidation as the lotus tubers mature in the field [11]. In previous studies, Nagashima et al. used atomic absorption spectrophotometry-based analysis to confirm that the main component of the black spots was iron (Fe) and suggested that over −100 mV of oxidation reduction potential (ORP) causes the blackening of lotus tubers due to the oxidation of Fe(II) by withholding the supply of oxygen from the lotus root [12,13]. Additionally, the authors speculated that the black spots' precipitants are Fe(III) oxide-hydroxide or FeS. However, the chemical characteristics (other than Fe) of black spots on the surface of the lotus tubers and the relationship to soil chemical parameters are still unknown. Furthermore, the relationship between the extent of the damage and the soil chemical characteristics has not yet been elucidated.

In addition, it is presumed that the invaded sites of the lotus tubers release several extracts [11] that can act as growth substrates for soil microorganisms; therefore, certain microbes may be involved in the blackening of the lotus tubers. In this study, to elucidate the blackening mechanisms of "*kurokawa-senchu-byo*", we performed a soil chemical analysis and evaluation of the disease level in the lotus cultivation fields, identified the chemical components of black spots on the lotus surface, and performed a 16S rRNA gene-based microbial community analysis of the black spots.

2. Materials and Methods

2.1. Sample Collection and Damage Index Evaluation

The soils and lotus tubers used in this study were obtained from a total of nine cultivation fields in the Ibaraki (IA–IH) and Niigata (NI) prefectures of Japan (Table 1). The lotus tuber damage from "*kurokawa-senchu-byo*" was evaluated on a scale from 0 to 4 according to the damage index used in a previous study [9]. IA–IH and NI samples were collected in 2020 and 2019, respectively. IC was a newly developed lotus cultivation field that was converted from a rice paddy field in 2018.

Table 1. Summary of lotus cultivation fields, damage index values of lotus tubers, and soil chemical analysis data.

Field	Field Size	Lotus	Damage Index	pH	EC	NH_4-N	P_2O_5	K_2O	CaO	MgO	SG [c]	TN	TC	C/N	CEC
Name	(m^2)	Cultivar	(0,1,2,3,4)	(-)	(dS/m)	(mg/100 g-Dry Soil)					(-)	(%)	(%)	(-)	(meq/100 g)
I [a] A-1 [b]	ca. 1000	"Koshuku"	2.42 ± 0.99 (31) [d]	5.8	0.44	5.3	34.8	28.8	383.6	110.2	0.39	0.48	4.81	10.1	27.5
IA-2	ca. 1000		2.60 ± 0.82 (25)	6.0	0.55	39.3	38.1	66.2	513.0	146.5	0.30	0.62	6.17	9.9	39.3
IB-1	ca. 1000		2.34 ± 1.29 (32)	6.0	0.56	13.7	58.9	54.6	418.8	133.1	0.43	0.49	5.03	10.3	26.1
IB-2	ca. 1000		2.07 ± 0.83 (27)	6.1	0.70	22.2	52.8	65.7	532.8	187.6	0.31	0.67	6.80	10.1	36.9
IC-1	ca. 1100	"Kanasumi No. 24"	0 (20)	6.3	0.18	20.7	10.2	56.1	349.0	73.4	0.68	0.38	3.94	10.4	24.0
IC-2	ca. 1100		0 (19)	6.8	0.14	23.4	23.9	65.4	278.0	71.2	1.04	0.35	2.88	8.3	18.6
ID-1	ca. 1000	"Power"	2.41 ± 0.94 (17)	6.7	0.59	68.1	71.4	66.5	635.1	104.3	0.32	0.66	6.53	10.0	36.8
ID-2	ca. 1000		2.42 ± 0.90 (12)	6.5	0.42	21.1	59.0	47.8	533.1	99.5	0.48	0.56	5.71	10.2	34.3
IE-1	ca. 1000	"Koshuku"	1.75 ± 0.79 (20)	5.8	0.47	13.7	29.4	42.1	394.0	69.4	0.48	0.48	4.96	10.3	27.6
IE-2	ca. 1000		1.52 ± 0.64 (27)	5.6	0.51	12.0	33.0	33.5	353.8	61.6	0.57	0.47	4.71	9.9	24.9
IF-1	ca. 1000	"Koshuku"	1.18 ± 0.90 (28)	6.0	0.28	9.6	33.3	46.0	302.4	53.4	0.67	0.39	4.01	10.3	21.4
IF-2	ca. 1000		1.90 ± 0.91 (20)	5.9	0.53	17.8	33.4	47.7	395.9	71.9	0.47	0.48	5.00	10.3	28.9
IG	ca. 2000	"Power"	2.67 ± 0.58 (3)	– [e]	–	–	–	–	–	–	–	–	–	–	–
IH	ca. 1000	"Matsukaze"	3.25 ± 0.50 (4)	–	–	–	–	–	–	–	–	–	–	–	–
NI	ca. 4000	"Daruma"	3.25 ± 0.47 (20)	–	–	–	–	–	–	–	–	–	–	–	–

[a] The first letter indicates the location of the fields. I: Ibaraki and N: Niigata. [b] The number indicates the duplicate samples from the different locations in the field. [c] Specific gravity. [d] Number of lotus tubers used for damage index evaluation. [e] Not determined.

2.2. Chemical and Microscopic Analyses

2.2.1. Cultivation Fields

The soil chemical analyses of the six lotus cultivation fields (IA, IB, IC, ID, IE, and IF) were performed immediately after sampling (Table 1). The pH (glass electrode method), electric conductivity (EC, glass electrode method), NH_4^+–N (indophenol and 1N KCl methods), effective phosphate (Truog procedure), potassium (flame photometry method), calcium carbonate (atomic absorption spectrometry method), magnesia (atomic absorption spectrometry method), total nitrogen (TN, dry combustion method), total carbon (TC, dry combustion method), and cation exchange capacity (CEC, Schollenberger method) were measured. Soil specific gravity (SG) was calculated by measuring the soil sample weight and dry soil sample weight.

2.2.2. Lotus Tubers and Black Spots

Lotus tubers exhibiting both black spots and healthy sections were obtained from lotus cultivation field NI. The sections were analyzed using scanning electron microscopy-energy dispersive X-ray spectroscopy (SEM-EDS, TM3030Plus, Hitachi, Tokyo, Japan). To quantify the phosphorus (P) and iron (Fe) in the black spot samples, we excised the entire black spot on the three lotus tuber surfaces from three cultivars (IA: "Koshuku"; IG: "Power"; and IH: "Matsukaze"), (Table 1). Equal amounts of healthy lotus tissue were also cut from the same lotus tubers. These dry weights were determined using an oven at 600 °C for 30 min. After measuring dry weights, P and Fe were eluted using 0.1 M HCl. The eluted solutions were analyzed using an inductively coupled plasma optical emission spectrometer (ICP–OES, ICPE-9820, Shimadzu, Kyoto, Japan).

2.3. 16S rRNA Gene Analysis

2.3.1. DNA Extraction, PCR Amplification, and 16S rRNA Gene Sequencing Analysis

Duplicate black-spot samples were obtained from two lotus tubers at field NI (Table 1). These samples were stored at −80 °C prior to DNA extraction. DNA extraction was performed using a FastDNA Spin Kit for Soil (MP Biomedicals, Santa Ana, CA, USA) according to the manufacturer's protocol. PCR amplification of the 16S rRNA gene was performed using the universal forward primer (Univ515F: 5′-GTGCCAGCMGCCGCGGTAA-3′) and the reverse primer (Univ909R: 5′-CCCCGYCAATTCMTTTRAGT-3′) [14]. PCR was performed according to the protocol used in a previous study [15]. PCR products were purified by a QIAquick PCR purification kit (Qiagen, Valencia, CA, USA) following the manufacturer's protocol. The purified 16S rRNA genes were sequenced using the MiSeq Reagent kit v3 and the MiSeq system (Illumina, San Diego, CA, USA). Raw 16S rRNA gene sequences were analyzed using QIIME 2 ver. 2021.4 [16]. Quality trimming, primer sequence removal, paired-end assembly, and a chimera check were performed using DADA2 [17]. After

the DADA2 treatment, the sequences were clustered at ≥97% similarity into operational taxonomic units (OTUs) using VSEARCH [18]. Taxonomic assignment was performed using classify-sklearn retained on the SILVA database version 138 [19]. Representative OTUs were chosen on the basis of the >1% average abundance rate.

2.3.2. Deposition of 16S rRNA Gene Sequence Data

The raw 16S rRNA gene sequences were deposited into the DDBJ Sequence Read Archive database (DRA012886). The 16S rRNA gene sequences of representative OTUs were deposited into the DDBJ/EMBL/GenBank databases (LC655158–LC655171).

3. Results

3.1. Survey and Chemical Analysis of the Lotus Cultivation Field

In this study, we collected soil and lotus tuber samples from six lotus cultivation fields and evaluated the damage index and soil chemical characteristics (Figure 1A–F). The damage index values ranged from 0 to 2.6, and the newly-developed field IC showed no disease occurrence by *H. diversa* (Table 1). Then, we performed a linear regression analysis to evaluate the correlation between the damage index and the soil chemical characteristics (Figure 1). The analyses revealed a positive linear relationship with a strong correlation between the damage index values and P_2O_5 (R^2 = 0.63), CEC (0.55), EC (0.63), CaO (0.55), TN (0.60), and TC (0.64), (Figure 1A–F), whereas there were weak or no correlations with the NH_4-N, K_2O, MgO, and C/N ratios. The specific gravity (SG) showed a strong negative correlation with the damage index values (0.74, Figure 1G). Soil chemical characteristics with positive linear relationships are contained in several fertilizers and calcium cyanamide. Study results suggest that these residual fertilizer components may influence the occurrence of "*kurokawa-senchu-byo*". In addition, the SG, which has a negative linear relationship, indicates that softer soils have greater damage index values than harder soils; thus, changes in SG properties may affect the mobility of *H. diversa* in soil. On the other hand, this study did not conduct soil chemical analysis at IG, IH, and NI fields; therefore, further investigation is required to determine a more accurate correlation between the damage index and soil chemical characteristics.

3.2. Chemical Analysis of Lotus Tubers Damaged by Hirschmanniella Diversa

We observed SEM-EDS images from sections exhibiting both black spots and healthy parts on the lotus tubers obtained from lotus cultivation field NI (Figure 2A,B). As a result, inorganic precipitation was observed on the black spots (Figure 2F) but not on the healthy parts (Figure 2C). Additionally, we confirmed that there were no nematodes around the black spots, which supports the previous observation that *H. diversa* prefers to invade young lotus tubers [11]. Furthermore, the EDS elemental map-sum spectrum of the healthy parts of the lotus tuber revealed that most of the elements were C (64.6% (*w*/*w*)) and O (32.7% (*w*/*w*)), while Fe, P, and other elements were broadly distributed (Figure 2G,H). On the other hand, P and Fe were concentrated on the sections containing black spots (Figure 2D,E). Comparison of elemental map-sum spectra showed that on the surface of healthy lotus tubers, Fe and P were 0.24% (*w*/*w*) and 0.09% (*w*/*w*), respectively, while the values in sections containing black spots were higher, with 1.68% (*w*/*w*) Fe and 0.12% (*w*/*w*) P.

The results of the SEM-EDS analysis indicated that the black spots on the lotus tuber surface were composed of phosphorus and iron. Therefore, we quantified the P and Fe concentrations of the black spots and healthy parts on the lotus surface from three different cultivars using ICP–OES (Figure 3). As a result, the P concentrations in the black spots ranged from 7.31–9.15 mg/g-dry, while those in the healthy parts ranged from 4.89–6.64 mg/g-dry (Figure 3A). Fe concentrations in the black spots and healthy parts were 0.95–4.09 mg/g-dry and 0.73–0.96 mg/g-dry, respectively (Figure 3B). The average P concentrations were significantly ($p < 0.05$) different between black spots (8.34 ± 0.94 mg/g-dry) and healthy parts (5.65 ± 0.87 mg/g-dry). For the Fe concentrations, the mean value found in the black

spots (2.35 ± 1.60 mg/g-dry) was 2.7-fold higher than that found in the healthy parts (0.87 ± 0.13 mg/g-dry), while the difference was not statistically significant ($p = 0.25$).

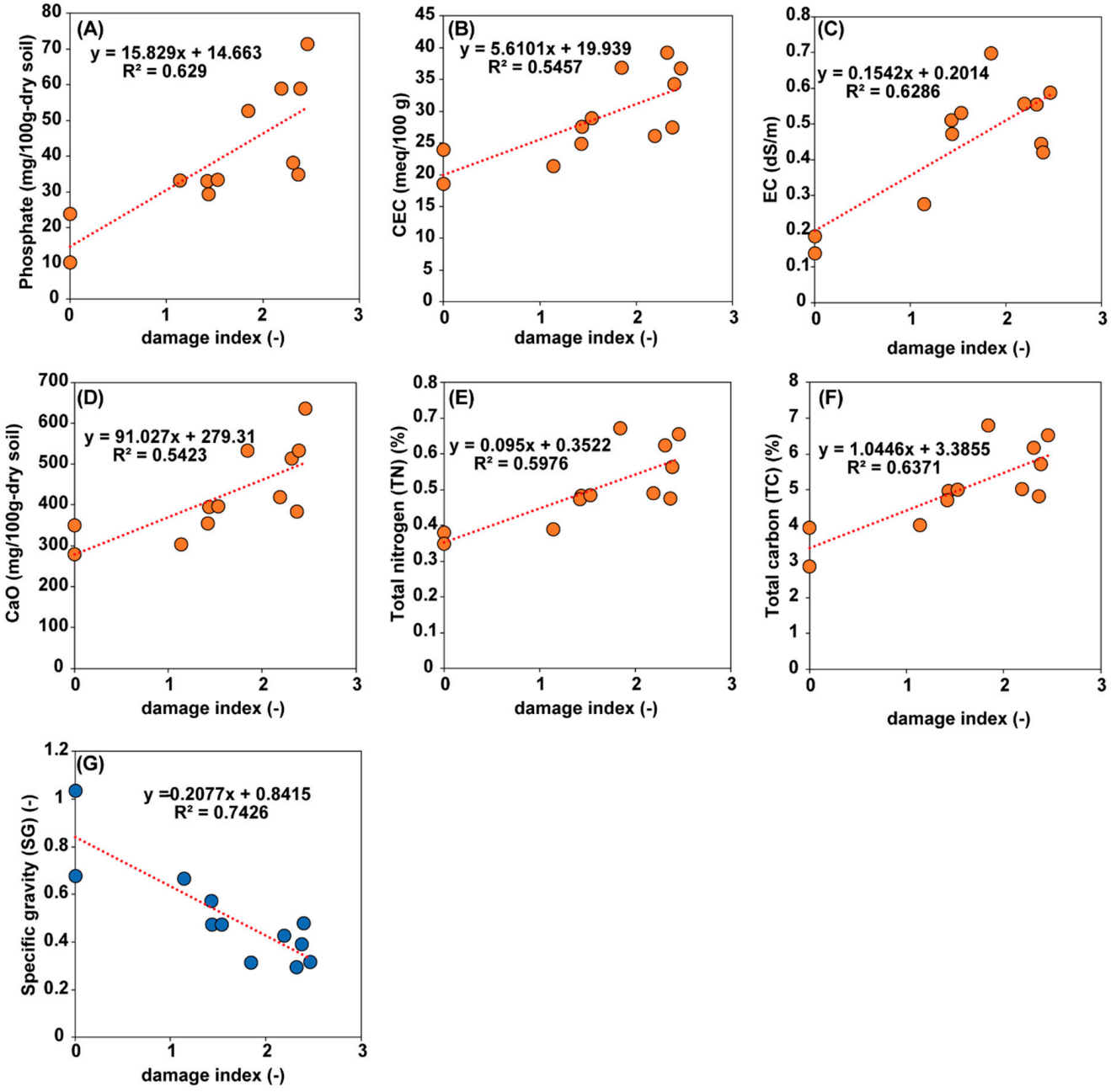

Figure 1. The calibration curve of damage index values in relation to soil chemical characteristics of (**A**) Phosphate (P_2O_5), (**B**) cation exchange capacity (CEC), (**C**) electric conductivity (EC), (**D**) CaO, (**E**) total nitrogen (TN), (**F**) total carbon (TC), and (**G**) specific gravity (SG) obtained by linear regression analysis.

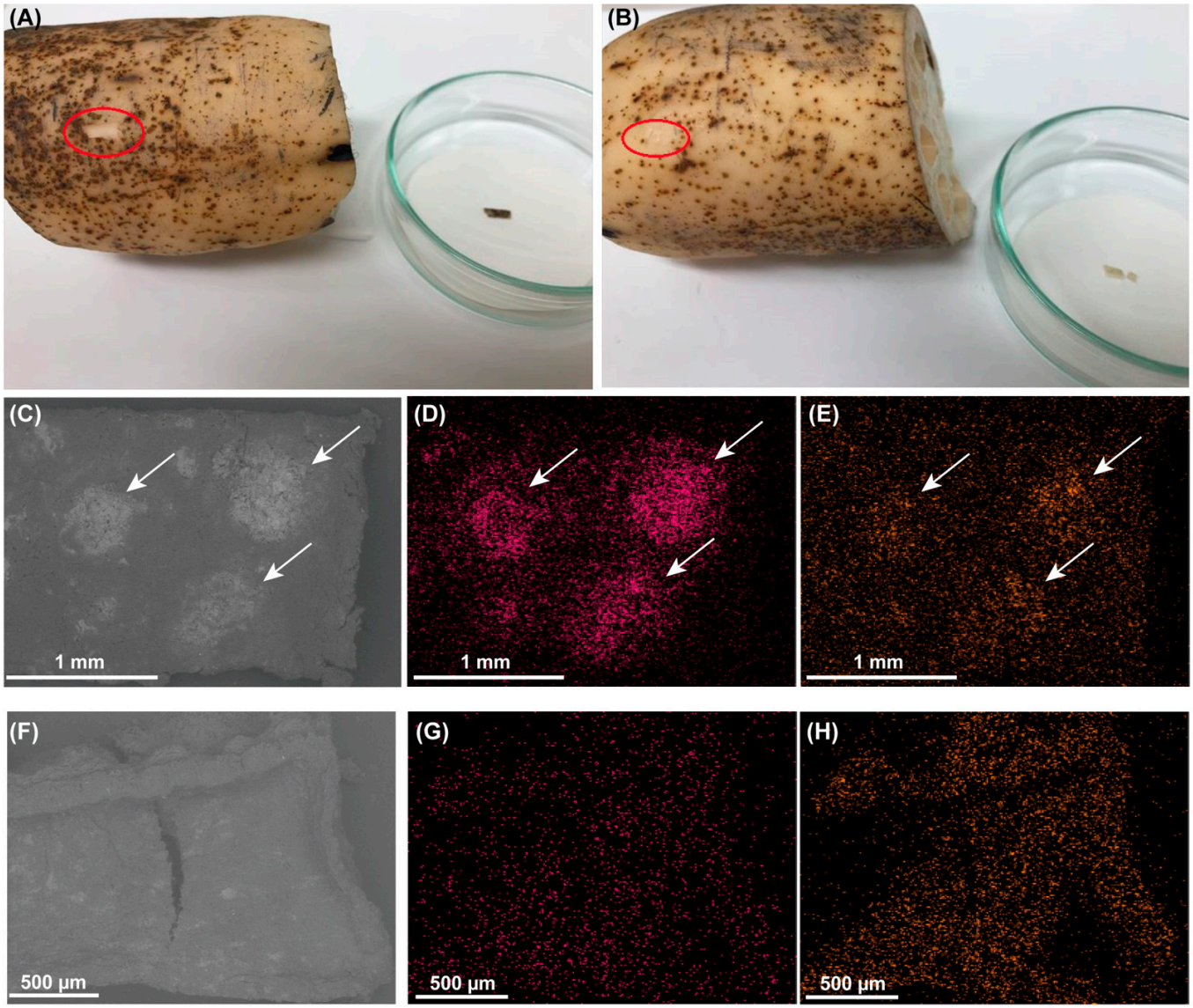

Figure 2. Photographic and scanning electron microscopy (SEM) images of sections of a lotus tuber. (**A**,**B**) are schematic images of collected sections of black spots and healthy parts of lotus tubers, respectively. (**C**–**E**) are sections of lotus tubers containing black spots. (**F**–**H**) are sections of healthy parts of lotus tubers. (**D**,**G**) are elemental maps of iron (Fe). (**E**,**H**) are elemental maps of phosphorus (P).

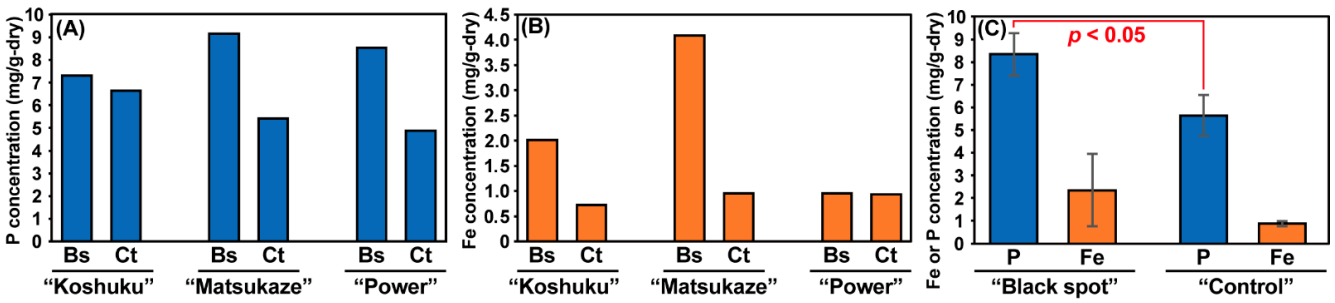

Figure 3. Concentrations of phosphorus (P) and iron (Fe) in the black spots (Bs) and healthy parts (Ct) of the lotus tuber surface. "Koshuku", "Matsukaze", and "Power" are different lotus cultivars. (**A**) P concentration, (**B**) Fe concentration, and (**C**) mean values of Fe and P concentrations in the Bs and Ct. The statistical analysis was performed based on Welch's *t*-test.

3.3. Microbial Community Analysis of Black Spots on the Lotus Tubers

To elucidate the blackening mechanisms relevant to microbial reactions, we performed a 16S rRNA gene sequence analysis of extracted DNA from the black spots obtained from lotus tubers in the NI cultivation field. We observed 26,416 average nonchimeric sequence reads after DADA2 treatment and 326 OTUs from two black-spot samples. Then, we removed eukaryotic 18S rRNA gene sequences derived from *N. nucifera* and red campion (*Silene dioica*) and observed 17,051 average sequence reads. At the OTU level, the predominant microorganisms were the families *Rhodocyclaceae* OTU001 (relative abundance rate 24.7%), *Rhodoferax* OTU002 (8.2%), *Geobacteraceae* OTU003 (7.8%), *Dechloromonas* OTU004 (5.1%), and *Methylotenera* OTU005 (3.7%), which are obligate methylotrophic bacteria (Figure 4). The most predominant microorganism, *Rhodocyclaceae* OTU001, is closely related to *Georgfuchsia toluolica* strain G5G6 (NR_115995.1) with 99% (372/376 bp) similarity, which reduces nitrate, MnO_2, and various Fe(III) species and degrades aromatic compounds (e.g., toluene, ethylbenzene, phenol, and benzaldehyde) [20]. In addition, *G. toluolica* cannot grow on sugars, hydrogens, or organic acids. Although the closest strain of *Rhodoferax* OTU002 is *Rhodoferax antarcticus* strain DSM 24876 (CP019240.1) at 100% similarity (374/374 bp), the bacterium is also closely related to *R. ferrireducens* strain RKAT120 (KU179848.1) of dissimilatory Fe(III)-reducing bacteria (DIRB) at 99% similarity (370/374 bp) [21]. *Geobacteraceae* OTU003 is related to *Pelobacter propionicus* strain DSM 2379 (NR_074975.1) at 99% similarity (375/376 bp), and the bacterium also has the capability of iron reduction with propionate and acetate production [22,23]. The closest strain of *Dechloromonas* OTU004 is *Dechloromonas hortensis* strain OX0627 (MG576023.1) at 99% similarity (375/376 bp), which is a chlorate-reducing, propionate- and acetate-oxidizing bacteria [24]. Thus, this study found that several DIRB and other reducing bacteria predominated in the black spots of lotus tubers.

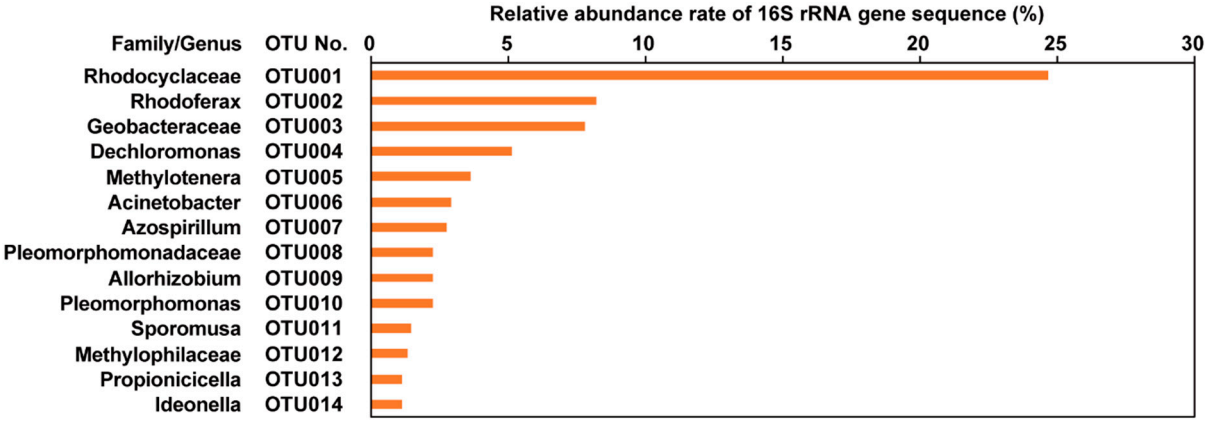

Figure 4. Relative abundance rate of predominant operational taxonomic units (OTUs) based on 16S rRNA gene sequences.

4. Discussion

In this study, we attempted to elucidate the blackening mechanisms of lotus tubers by analyzing their chemical and microbial characteristics. Based on the linear relationship between the damage index and phosphate concentration in the lotus cultivation fields, along with SEM-EDS/ICP–OES analyses, we found that P and Fe were concentrated in the black spots of lotus tubers (Figures 2 and 3), suggesting that the black spots were caused by the formation of P-Fe compounds. To date, vivianite [$Fe_3(PO_4)_2{\cdot}8H_2O$], as an iron phosphate mineral, has been frequently found in sediments and organic soils under reducing (anaerobic) conditions [25,26]. Vivianite is stably present in rice paddy soil and forms under reducing conditions when PO_4^{3-} and Fe^{2+} concentrations are sufficient and S^{2-} concentrations are low [26,27]. In addition, the ORP of lotus cultivation soil (−170 mV) is known to be similar to that of rice paddy soils (from −112 to −187 mV) [24], and the soil has been used for isolating sources of Fe(III)-reducing bacteria [28]. Vivianite is originally

a colorless mineral, but when exposed to air, the iron is oxidized, and vivianite exhibits several colors, such as blue-green and black [29]. Nanzyo et al. confirmed the presence of vivianite minerals in rice roots, accounting for 25–29% of the total root P [30]. In addition, Nanzyo reported that a 0.1 g P_2O_5/kg plant-available P level in the plowing layer of the soil is an important condition for the detection of vivianite in rice roots [26]. Thus, assuming that the black spots of lotus tubers are vivianite, all lotus cultivation fields in this study have >0.1 g P_2O_5/kg plant-available P levels (Table 1), indicating that the environments are suitable for the formation of vivianite.

Using 16S rRNA gene analysis, we found that DIRB and other reducing bacteria were predominantly present in the black spots of lotus tubers (Figure 4). It has been reported that several organic carbon-oxidizing and Fe(III)-reducing DIRB can induce the precipitation of minerals such as vivianite, siderite, apatite, and magnetite [25,31,32]. A recent study revealed that vivianite is formed by the reduction of Fe(III), using activated sludge under anaerobic conditions, and *Rhodoferax* sp. and *Dechloromonas* sp. involved in the iron cycles were predominant in the sludge after vivianite formation [33]. In addition, batch experiments using *Geobacter sulfurreducens* of the family *Geobacteraceae* for P recovery from sewage have also revealed that sufficient PO_4^{3-} promotes cell growth, leading to higher Fe^{3+} reduction and vivianite yield [34]. Thus, it is possible that *Rhodocyclaceae* OTU001, *Rhodoferax* OTU002, and *Geobacteraceae* OTU003, which are predominant DIRBs in the black spots of lotus tubers, can form or induce iron phosphate minerals such as vivianite by reducing Fe^{3+} in lotus-cultivation soils. The most predominant OTU001 is closely related to *G. toluolica* of DIRB, which can degrade toluene, ethylbenzene, phenol, p-cresol, m-cresol, benzaldehyde, and p-hydroxybenzoate [20]. It has been reported that phenolic compounds are abundant in lotus tubers [35]. Therefore, it is likely that *Rhodocyclaceae* OTU001 utilizes aromatic compounds, such as phenol leached from damaged parts of lotus tubers by *H. diversa,* and reduces Fe(III). Recently, vivianite formation mechanisms using microbial reactions via extracellular electron transfer have been proposed [29,36]. First, under anaerobic conditions, P (mainly HPO_4^{2-} and PO_4^{3-}) is adsorbed on the surface of Fe(III) oxides or coprecipitated with Fe^{3+} in the liquid phase to form $FePO_4$. Then, DIRB reduces Fe(III) oxides, and $FePO_4$ releases PO_4^{3-} by providing H^+ through organic compound degradation. Finally, vivianite is formed by a chemical reaction with Fe^{2+}, PO_4^{3-}, and H_2O. Assuming that the P and Fe compounds detected in this study are from vivianite, it is presumed that substrates supplied by the damaged spots of lotus tubers are used as electron donors, and Fe(III) in lotus-cultivation soils is reduced, leading to the formation of black spots on the surface of lotus tubers.

In summary, we propose the blackening mechanism of lotus tubers under the assumption of vivianite as a source of black spot minerals (Figure 5). First, after the lotus tubers are planted in the fields, *H. diversa* immediately invades the young lotus tubers [11]. After damaging the young lotus tubers, several substrates are eluted from damaged parts of the lotus tubers as the hole expands due to growth and maturation. Then, DIRB, mainly OTU001, OTU002, and OTU003, oxidizes the leached substrates (e.g., aromatic compounds and organic acids) with Fe(III) reduction and forms Fe^{2+} and PO_4^{3-}. Finally, black spots are formed by the reprecipitation of these compounds. On the other hand, in this study, we were not able to accurately identify the chemical compounds of the black spots. In addition, microbiological findings are at the microbial community structure level; therefore, it is necessary to confirm the reproductivity of P-Fe minerals, such as vivianite, using culture-based experiments. This study is the first to identify the chemical compounds and microbial community structures of black spots on lotus tubers, and it is hoped that the elucidation of the blackening mechanisms will be helpful for "*kurokawa-senchu-byo*" control.

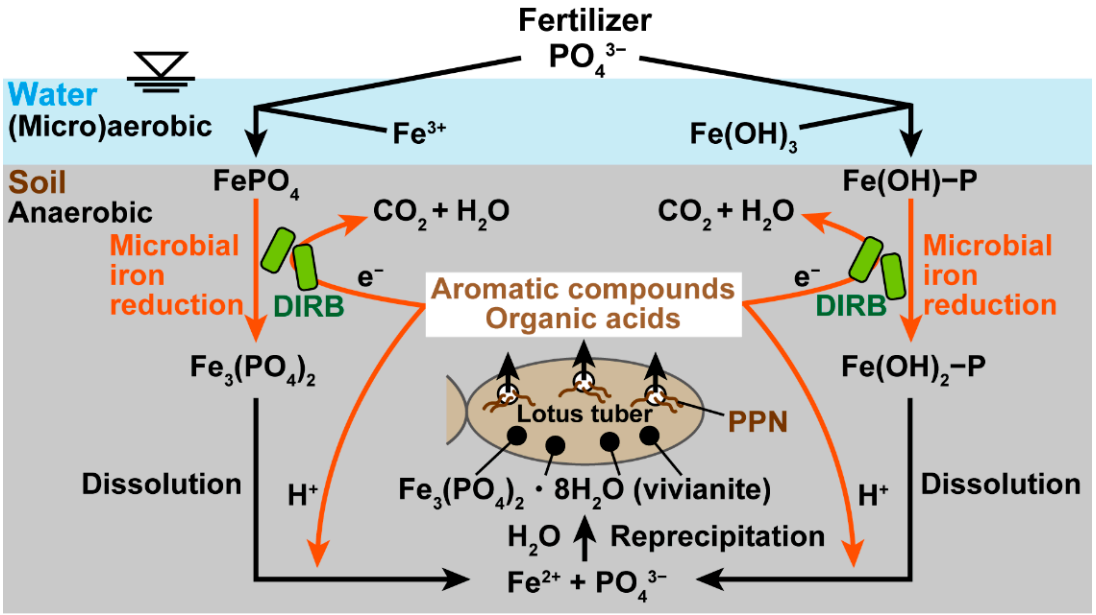

Figure 5. Hypothesis of the black spot formation process in lotus cultivation fields. DIRB and PPN are dissimilatory Fe(III)-reducing bacteria and plant parasitic nematodes, respectively. White circles on the lotus tuber indicate parts damaged by PPN before vivianite reprecipitation, which elute several substrates into the soil. Orange arrows and lines indicate biological processes. Black arrows and lines indicate chemical and physical processes.

5. Conclusions

In this study, to clarify the blackening mechanism of "*kurokawa-senchu-byo*", we performed a soil chemical analysis and an evaluation of the disease level in the lotus cultivation fields, identified the chemical components of black spots on the lotus surface, and performed a 16S rRNA gene-based microbial community analysis of the black spots. The linear regression analyses between damage index and soil chemical characteristics showed that the damage index had a strong positive linear relationship with some fertilizer components (P_2O_5, CEC, EC, CaO, TN, and TC). As a result of the SEM-EDS analysis, we confirmed that Fe and P were co-precipitated on the black spots in the lotus tuber. ICP-OES analysis showed that the average P concentrations in the black spots were significantly ($p < 0.05$) higher than in the healthy parts, and average Fe concentration in the black spots showed a 2.7-fold higher value compared with healthy parts. The 16S rRNA gene analysis revealed that DIRB was predominant in the black spots, suggesting that these bacteria are important to the formation of P and Fe compounds in black spots. Consequently, this study is the first to identify the chemical compounds and microbial community structures of black spots on lotus tubers, and it is hoped that the elucidation of the blackening mechanisms will be helpful for "*kurokawa-senchu-byo*" control.

Author Contributions: Conceptualization, K.K. and H.K.; methodology, K.K., H.K., S.M. and T.S.; software, K.K.; validation, K.K., H.K., S.M. and M.G.; formal analysis, K.K. and H.K.; investigation, K.K., H.K., S.M., T.S., M.T., M.G. and T.K.; resources, K.K., H.K., S.M., T.S., M.T., M.G. and T.K.; data curation, K.K., H.K., S.T. and T.N.; writing—original draft preparation, H.K. and K.K.; writing—review and editing, K.K., S.M., M.T., M.G., T.K., M.H., T.Y., S.T. and T.N.; visualization, K.K., H.K., S.M., T.S., M.G. and T.N.; supervision, K.K., M.H., T.Y. and T.N.; project administration, K.K.; funding acquisition, K.K. All authors have read and agreed to the published version of the manuscript.

Funding: This research was funded by the Japan Society for the Promotion of Science (JSPS) KAKENHI, grant number 19KT0015.

Institutional Review Board Statement: Not applicable.

Informed Consent Statement: Not applicable.

Data Availability Statement: Not applicable.

Acknowledgments: The authors thank Riho Tokizawa at the National Institute of Advanced Industrial Science and Technology (AIST) for her technical assistance. The authors also thank Nobuo Saito at the Analysis Center, the Nagaoka University of Technology, for SEM-EDS and ICP–OES analyses.

Conflicts of Interest: The authors declare no conflict of interest.

References

1. Kurashita, H.; Kuroda, K.; Narihiro, T.; Takagi, M.; Goto, M.; Ikeda, S.; Hirakata, Y.; Hatamoto, M.; Maki, S.; Yamaguchi, T.; et al. Accurate evaluation of blackening disease in lotus (*Nelumbo nucifera* Gaertn.) using a quantitative PCR-based assay for *Hirschmanniella diversa* Sher and *H. imamuri* Sher. *Crop Prot.* **2021**, *139*, 105380. [CrossRef]
2. Lu, H.-F.; Tan, Y.-W.; Zhang, W.-S.; Qiao, Y.-C.; Campbell, D.E.; Zhou, L.; Ren, H. Integrated emergy and economic evaluation of lotus-root production systems on reclaimed wetlands surrounding the Pearl River Estuary, China. *J. Clean. Prod.* **2017**, *158*, 367–379. [CrossRef]
3. Mihira, T. Browning tuber disease of Indian lotus *Nelumboi nucifera*, Kurokawa-senchu-byo caused by rice root nematode, *Hirschmanniella imamuri*. *Bull. Chiba Prefect. Agric. Res. Cent.* **2002**, *1*, 121–124.
4. Takagi, M.; Goto, M.; Wari, D.; Kashima, T.; Toyota, K. Seasonal occurrence and life cycle of lotus root nematode *Hirschmanniella diversa* (Tylenchida: Pratylenchidae) in lotus roots in paddy fields. *Appl. Entomol. Zool.* **2019**, *54*, 465–471. [CrossRef]
5. Jeger, M.; Bragard, C.; Caffier, D.; Candresse, T.; Chatzivassiliou, E.; Dehnen-Schmutz, K.; Gilioli, G.; Grégoire, J.C.; Anton, J.; Miret, J.; et al. Pest categorisation of *Hirschmanniella* spp. *EFSA J.* **2018**, *16*, e05297. [CrossRef] [PubMed]
6. Koyama, Y.; Thar, S.P.; Kizaki, C.; Toyota, K.; Sawada, E.; Abe, N. Development of specific primers to *Hirschmanniella* spp. causing damage to lotus and their economic threshold level in Tokushima prefecture in Japan. *Nematology* **2013**, *15*, 851–858. [CrossRef]
7. Takagi, M.; Goto, M.; Hisatsune, K.; Kashima, T. Evaluation of weeds and wild lotus in and around lotus paddy fields in Ibaraki prefecture as possible alternative host plants of the lotus root nematode, *Hirschmanniella diversa* (Tylenchida: Pratylenchidae) causing damages to lotus, *Nelumbo nucifera*. *Annu. Rep. Kanto-Tosan Plant Prot. Soc.* **2016**, *63*, 98–101. [CrossRef]
8. Uematsu, S.; Yabu, T.; Mitsuyoshi, Y.; Kurihara, T.; Koga, H. Light and scanning electron microscopy of the Indian lotus roots invaded by *Hirschmanniella diversa*. *Nematol. Res.* **2016**, *46*, 79–82. [CrossRef]
9. Takagi, M.; Goto, M.; Wari, D.; Saito, M.; Perry, R.; Toyota, K. Screening of Nematicides against the Lotus Root Nematode, *Hirschmanniella diversa* Sher (Tylenchida: Pratylenchidae) and the Efficacy of a Selected Nematicide under Lotus Micro-Field Conditions. *Agronomy* **2020**, *10*, 373. [CrossRef]
10. Takagi, M.; Ogawara, T.; Toyota, K. The new integrated pest management system incorporating benfuracarb granule against lotus root nematode *Hirschmanniella diversa*. *Plant Prot.* **2020**, *74*, 22–26.
11. Uematsu, S.; Yabu, T.; Yao, M.; Kurihara, T.; Koga, H. Ultrastructure of *Hirschmanniella diversa* early-stage infection in browning rhizomes of Indian lotus. *J. Nematol.* **2020**, *52*, e2020-55. [CrossRef]
12. Nagashima, T.; Toda, A.; Higashi, T. Relationship between the occurrence of epidermic blackening and browning of lotus rhizome, and redox state in the plow layer at lotus field–Fundamental studies on the land consolidation of lotus field (I). *Trans.-Jpn. Soc. Irrig. Drain. Reclam. Eng.* **1997**, *189*, 81–88. [CrossRef]
13. Nagashima, T.; Toda, A.; Higashi, T. A Study on the Properties of Soil in the Plow Layer of Lotus Field, and Effect of some Conditions to its Redox State-Fundamental studies on the land consolidation of lotus field (II). *Trans. Jpn. Soc. Irrig. Drain. Reclam. Eng.* **1997**, *189*, 89–96. [CrossRef]
14. Kozich, J.J.; Westcott, S.L.; Baxter, N.T.; Highlander, S.K.; Schloss, P.D. Development of a Dual-Index Sequencing Strategy and Curation Pipeline for Analyzing Amplicon Sequence Data on the MiSeq Illumina Sequencing Platform. *Appl. Environ. Microbiol.* **2013**, *79*, 5112–5120. [CrossRef] [PubMed]
15. Kuroda, K.; Kurashita, H.; Arata, T.; Miyata, A.; Kawazoe, M.; Nobu, M.K.; Narihiro, T.; Ohike, T.; Hatamoto, M.; Maki, S.; et al. Influence of Green Tuff Fertilizer Application on Soil Microorganisms, Plant Growth, and Soil Chemical Parameters in Green Onion (*Allium fistulosum* L.) Cultivation. *Agronomy* **2020**, *10*, 929. [CrossRef]
16. Bolyen, E.; Rideout, J.R.; Dillon, M.R.; Bokulich, N.A.; Abnet, C.C.; Al-Ghalith, G.A.; Alexander, H.; Alm, E.J.; Arumugam, M.; Asnicar, F.; et al. Reproducible, interactive, scalable and extensible microbiome data science using QIIME 2. *Nat. Biotechnol.* **2019**, *37*, 852–857. [CrossRef]
17. Callahan, B.J.; McMurdie, P.J.; Rosen, M.J.; Han, A.W.; Johnson, A.J.A.; Holmes, S.P. DADA2: High-resolution sample inference from Illumina amplicon data. *Nat. Methods* **2016**, *13*, 581–583. [CrossRef] [PubMed]
18. Rognes, T.; Flouri, T.; Nichols, B.; Quince, C.; Mahé, F. VSEARCH: A versatile open source tool for metagenomics. *PeerJ* **2016**, *4*, e2584. [CrossRef]
19. Yilmaz, P.; Parfrey, L.W.; Yarza, P.; Gerken, J.; Pruesse, E.; Quast, C.; Schweer, T.; Peplies, J.; Ludwig, W.; Glöckner, F.O. The SILVA and "All-species Living Tree Project (LTP)" taxonomic frameworks. *Nucleic Acids Res.* **2014**, *42*, D643–D648. [CrossRef]
20. Weelink, S.A.B.; van Doesburg, W.; Saia, F.T.; Rijpstra, W.I.C.; Röling, W.F.M.; Smidt, H.; Stams, A.J.M. A strictly anaerobic betaproteobacterium *Georgfuchsia toluolica* gen. nov., sp. nov. degrades aromatic compounds with Fe(III), Mn(IV) or nitrate as an electron acceptor. *FEMS Microbiol. Ecol.* **2009**, *70*, 575–585. [CrossRef] [PubMed]

21. Finneran, K.T.; Johnsen, C.V.; Lovley, D.R. *Rhodoferax ferrireducens* sp. nov., a psychrotolerant, facultatively anaerobic bacterium that oxidizes acetate with the reduction of Fe(III). *Int. J. Syst. Evol. Microbiol.* **2003**, *53*, 669–673. [CrossRef] [PubMed]
22. Lonergan, D.J.; Jenter, H.L.; Coates, J.D.; Phillips, E.J.P.; Schmidt, T.M.; Lovley, D.R. Phylogenetic analysis of dissimilatory Fe(III)-reducing bacteria. *J. Bacteriol.* **1996**, *178*, 2402–2408. [CrossRef] [PubMed]
23. Schink, B. Fermentation of 2,3-butanediol by *Pelobacter carbinolicus* sp. nov. and *Pelobacter propionicus* sp. nov., and evidence for propionate formation from C2 compounds. *Arch. Microbiol.* **1984**, *137*, 33–41. [CrossRef]
24. Wolterink, A.; Kim, S.; Muusse, M.; Kim, I.S.; Roholl, P.J.M.; van Ginkel, C.G.; Stams, A.J.M.; Kengen, S.W.M. *Dechloromonas hortensis* sp. nov. and strain ASK-1, two novel (per)chlorate-reducing bacteria, and taxonomic description of strain GR-1. *Int. J. Syst. Evol. Microbiol.* **2005**, *55*, 2063–2068. [CrossRef] [PubMed]
25. Rothe, M.; Kleeberg, A.; Hupfer, M. The occurrence, identification and environmental relevance of vivianite in waterlogged soils and aquatic sediments. *Earth-Sci. Rev.* **2016**, *158*, 51–64. [CrossRef]
26. Nanzyo, M.; Kanno, H. *Inorganic Constituents in Soil: Basics and Visuals*; Springer Nature: Basingstoke, UK, 2018; ISBN 9789811312144.
27. Nriagu, J.O. Stability of vivianite and ion-pair formation in the system $fe_3(PO_4)_2$-$H_3PO_4H_3PO_4$-H_2o. *Geochim. Cosmochim. Acta* **1972**, *36*, 459–470. [CrossRef]
28. Viulu, S.; Nakamura, K.; Okada, Y.; Saitou, S.; Takamizawa, K. *Geobacter luticola* sp. nov., an Fe(III)-reducing bacterium isolated from lotus field mud. *Int. J. Syst. Evol. Microbiol.* **2013**, *63*, 442–448. [CrossRef] [PubMed]
29. Yuan, Q.; Wang, S.; Wang, X.; Li, N. Biosynthesis of vivianite from microbial extracellular electron transfer and environmental application. *Sci. Total Environ.* **2021**, *762*, 143076. [CrossRef] [PubMed]
30. Nanzyo, M.; Onodera, H.; Hasegawa, E.; Ito, K.; Kanno, H. Formation and Dissolution of Vivianite in Paddy Field Soil. *Soil Sci. Soc. Am. J.* **2013**, *77*, 1452–1459. [CrossRef]
31. Glasauer, S.; Weidler, P.G.; Langley, S.; Beveridge, T.J. Controls on Fe reduction and mineral formation by a subsurface bacterium. *Geochim. Cosmochim. Acta* **2003**, *67*, 1277–1288. [CrossRef]
32. O'Loughlin, E.J.; Boyanov, M.I.; Flynn, T.M.; Gorski, C.A.; Hofmann, S.M.; McCormick, M.L.; Scherer, M.M.; Kemner, K.M. Effects of bound phosphate on the bioreduction of lepidocrocite (γ-FeOOH) and maghemite (γ-Fe_2O_3) and formation of secondary minerals. *Environ. Sci. Technol.* **2013**, *47*, 9157–9166. [CrossRef] [PubMed]
33. Wang, R.; Wilfert, P.; Dugulan, I.; Goubitz, K.; Korving, L.; Witkamp, G.J.; van Loosdrecht, M.C.M. Fe(III) reduction and vivianite formation in activated sludge. *Sep. Purif. Technol.* **2019**, *220*, 126–135. [CrossRef]
34. Wang, S.; An, J.; Wan, Y.; Du, Q.; Wang, X.; Cheng, X.; Li, N. Phosphorus Competition in Bioinduced Vivianite Recovery from Wastewater. *Environ. Sci. Technol.* **2018**, *52*, 13863–13870. [CrossRef] [PubMed]
35. You, J.S.; Lee, Y.J.; Kim, K.S.; Kim, S.H.; Chang, K.J. Ethanol extract of lotus (*Nelumbo nucifera*) root exhibits an anti-adipogenic effect in human pre-adipocytes and anti-obesity and anti-oxidant effects in rats fed a high-fat diet. *Nutr. Res.* **2014**, *34*, 258–267. [CrossRef] [PubMed]
36. Li, R.H.; Cui, J.L.; Li, X.D.; Li, X.Y. Phosphorus Removal and Recovery from Wastewater using Fe-Dosing Bioreactor and Cofermentation: Investigation by X-ray Absorption Near-Edge Structure Spectroscopy. *Environ. Sci. Technol.* **2018**, *52*, 14119–14128. [CrossRef] [PubMed]